Quantifying Motor Skills in Early-Stage Parkinson's Disease Using Human Controller Modeling

Pool, Daan M.; de Vries, Rick J.; Pel, Johan J.M.

DOI
10.1016/j.ifacol.2022.10.238

Publication date
2022

Document Version
Final published version

Published in
IFAC-PapersOnline

Available online at www.sciencedirect.com

ScienceDirect

IFAC PapersOnLine 55-29 (2022) 96–101

Quantifying Motor Skills in Early-Stage Parkinson's Disease Using Human Controller Modeling

Daan M. Pool, * **Rick J. de Vries,** * **and Johan J.M. Pel** **

* *Control and Simulation Section, Aerospace Engineering, Delft University of Technology, Delft, The Netherlands (e-mail: d.m.pool@tudelft.nl).*

** *Vestibular and Oculomotor Research Group, Dept. of Neuroscience, Erasmus MC, Rotterdam, The Netherlands (e-mail: j.pel@erasmusmc.nl).*

Abstract: This paper investigates the potential of using a manual pursuit tracking task for quantifying loss of motor skills due to Parkinson's disease (PD), by applying human controller (HC) modeling techniques. With this approach, it is possible to obtain detailed quantitative data on motor performance in terms of control gain, response delay, stiffness and damping. Pursuit tracking data was collected from seven early-stage PD patients and a matched control group at the Erasmus MC in Rotterdam. Tracking performance was significantly worse in the PD group compared to the controls. Furthermore, the PD patients showed significantly lower control gains and degraded neuromuscular damping and bandwidth, which indicates that early-stage PD is associated with loss of quick and fast arm movements. While the PD patients showed less consistent and linear control behavior in the task, their data could still be modelled at high accuracy. Using HC models to quantify PD patients' fine motor skill abilities may contribute to improved (early) detection of motor skill loss in PD, as well as detailed monitoring of symptom development and intervention effectiveness.

Keywords: cybernetics, human controller modeling, motor skills, Parkinson's disease, medicine

1. INTRODUCTION

Parkinson's disease (PD) is a progressive age related disorder. The incidence levels rapidly increase in populations over 60 years. In PD, the Basal Ganglia (BG), which are crucial for motor control, do not function well due to a lack of dopamine. As a result, the cortex is unable to smoothly orchestrate motor behaviours, which leads to delays in various motor loops. Hence, motor symptoms, such as such as tremor, hypokinesia, rigidity and an impaired balance (De Lau and Breteler, 2006; Goetz et al., 2007) in initial stages, and severe motor complications in more advanced stages, are characteristic for PD (Jellinger, 2001). As it is especially the lost motor skills that are targeted with (dopaminergic) treatments (Gelb et al., 1999), detailed quantification of PD patients' motor skills is crucial for early detection and effective personalized care.

To date, clinical decision making relies on a combination of observations, (hetero)-anamnesis, and semi-structured tests, such as the Unified Parkinson's Disease Rating Scale (UPDRS) (Goetz et al., 2007). This provides neurologists with a good yet global insight into motor symptoms, which is generally quantified using a low-resolution (5 point) scale (Hoehn and Yahr, 1967). A more sensitive quantification of motor performance would improve insight into trends in motor symptom development and (short-term) effects of treatments. Recently, eye-hand coordination tests have been developed that show the clinical potential of assessing visuomotor deficits in early-stage PD (De Boer et al., 2013; Muilwijk et al., 2013), where significant delays in eye and hand movements were observed during goal-directed and behavioral inhibition tasks.

In this study, we focus on the use of *tracking tasks* for the further quantification of motor skill loss in PD. In a tracking task, a participant is asked to minimize a tracking error presented on a visual display. Performance in such a task directly depends on the integrity of the visuomotor system, i.e., eye-hand coordination skills. Tracking tasks have a unique potential for quantifying human controllers' (HC) dynamics using system identification techniques and mathematical modeling (McRuer and Jex, 1967; Mulder et al., 2018). Such methods allow for separating different physical aspects of HC behavior – e.g., control gain, response delay, and neuromuscular system (NMS) characteristics – and provide a quantification of human behavior on a very high resolution scale. While numerous experiments in which PD patients performed tracking tasks have been conducted (Flowers, 1978; Jones and Donaldson, 1989; Hufschmidt and Lücking, 1995; Jones et al., 1996; Soliveri et al., 1997), no HC modeling techniques were applied for explicit quantification of any degraded motor skills in PD.

This paper explores the potential of HC modeling techniques for detailed analysis of PD patients' motor skills measured in a tracking task. A set of pursuit tracking data collected from seven PD patients (P) and an age- and

10.1016/j.ifacol.2022.10.238

gender-matched control group (C) is presented. Tracking performance, control effort, and HC modeling results are explicitly compared between patients and controls.

2. METHODS

2.1 Control task

The control task selected for this study was a lateral target-tracking task with a pursuit display, similar to the tasks considered in previous experiments with PD patients (Flowers, 1978; Hufschmidt and Lücking, 1995; Soliveri et al., 1997). The pursuit display and a block diagram of the task are shown in Figures 1 and 2, respectively.

In this task, the pursuit display (see Fig. 1) presents the HC with continuous feedback of the to-be-followed target signal f_t (blue ring), the current position of the controlled system y (red filled circle). The lateral offset between both markers is the tracking error e, defined as $e = f_t - y$. The task of the HC is to keep the error e as small as possible by giving control inputs u with a side stick (see Section 2.2). Thus, the goal is to continuously position the red circle on the moving blue circle as accurately as possible. The controlled system dynamics H_{ce} were set to a single integrator (velocity control). The controlled element gain was set so that participants would never reach the stick deflection limits, i.e., $H_{ce}(s) = 2/s$.

As shown in Fig. 2, for pursuit tracking tasks with single integrator dynamics it is known that HCs' control is based on feedback of the error only (Vos et al., 2014; Mulder et al., 2019). This means that the additional feedbacks of f_t and y are not used for control. Therefore, H_{hc} in this task can be modeled as a single-input-single-output system, with dynamics as shown in Fig. 2 (McRuer and Jex, 1967; Vos et al., 2014). The HC dynamics

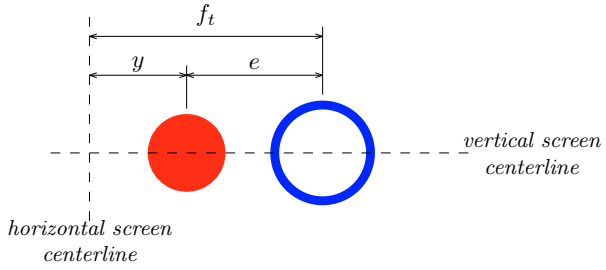

Fig. 1. Tracking task display.

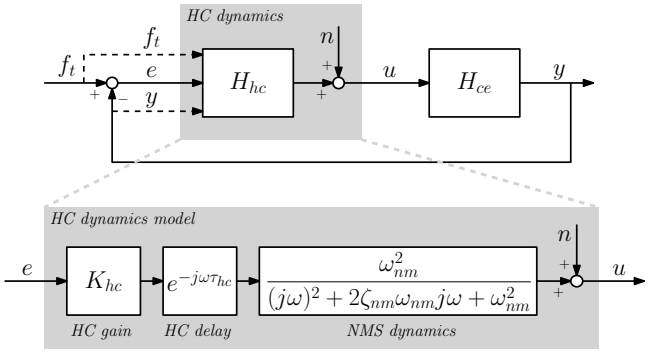

Fig. 2. Block diagram representation of the pursuit tracking task and the HC dynamics.

Fig. 3. A participant seated in the measurement setup consisting of a screen (1), a joystick (2), an infrared eye tracking system (3), and a chin rest (4).

model consists of an HC gain (K_{hc}) that captures the strength of HCs' responses to e, an HC delay (τ_{hc}), and the neuromuscular system (NMS) dynamics. For tracking tasks, these NMS dynamics are typically modeled as an underdamped second-order system with natural frequency ω_{nm} and damping ratio ζ_{nm} (Mulder et al., 2018).

2.2 Apparatus

The experiment was performed in the eye-hand coordination test setup at the Erasmus Medical Center (EMC) in Rotterdam also used by Muilwijk et al. (2013) and De Boer et al. (2014), see Fig. 3. Participants were seated in front of a 32-inch screen (ELO touch systems, Leuven, Belgium) on which the pursuit display of Fig. 1 was presented. Participants were asked to position their head on a chin rest to ensure minimal head movement. Though not reported on in this paper, the gaze of the eyes was registered throughout the experiment using an infrared video eye tracking system (Chronos Vision, Berlin, Germany). For the tracking task, a customized HOTAS Warthog joystick (Thrustmaster, Hillsboro, Oregon, USA) was added to the setup. To facilitate fine control inputs, the main spring was removed from the stick to reduce break-out force and stiffness, and a light custom grip was used.

2.3 Participants

Up to the time of writing of this paper, seven PD patients (3F, 4M) and an age and gender-matched control group were recruited from the department of Neurology of the EMC, see Table 1. Age ranged from 51-78 years ($\mu = 65.3$ years, $\sigma = 8.1$ years) for the PD patients and from 51-69 years ($\mu = 59.4$ years, $\sigma = 5.6$ years) for the healthy control group. Prior to participating, all subjects signed a written consent form. The study was approved by the research ethics committees of the EMC and TU Delft.

The inclusion criteria were similar to those used by De Boer et al. (2014). Cognitive functioning was assessed using the *Mini Mental State Examination* (MMSE) questionnaire (Folstein et al., 1975). Furthermore, frontal function deficits were tested with the *Frontal Assessment Battery* (FAB) (Dubois et al., 2000). Only subjects who had 'none' to 'mild' cognitive decline (MMSE $\geq$ 21) and had no or limited frontal function deficits (FAB $\geq$ 13) were included. No significant differences in MMSE and

Table 1. Participant details.

control	age	sex	MMSE	FAB	H&Y
1	51	f	30	17	-
2	59	m	30	18	-
3	60	f	30	16	-
4	63	m	30	18	-
5	56	f	28	18	-
6	69	m	30	18	-
7	58	m	30	18	-
patient	age	sex	MMSE	FAB	H&Y
1	67	m	30	15	II
2	65	f	29	17	I
3	51	m	26	15	II
4	62	f	29	18	0-I
5	78	m	23	16	II
6	69	m	28	18	I
7	65	f	21	17	I

FAB were present between the early-stage patients and the controls. Finally, the general motor function of the patients was assessed with part III of the *Movement Disorders Society Unified Parkinson's Disease Rating Scale* (MDS-UPDRS) (Goetz et al., 2007). From the MDS-UPDRS a Hoehn and Yahr (1967) (H&Y) stage was determined and patients with a score above III were excluded.

2.4 Experiment Procedures

Upon arrival, subjects completed the MMSE and FAB questionnaires. Thereafter they were asked to perform several eye-hand coordination tasks, including the tapping tasks of Muilwijk et al. (2013) and De Boer et al. (2013), as well as our tracking task. The time needed for the complete experiment was on average sixty minutes.

For the tracking task, participants first performed a single familiarization run without the target signal ($f_t = 0$), to familiarize themselves with the setup and the dynamics of the controlled system. Then, participants were asked to perform a total of eight 50-second tracking runs of the pursuit task. A performance score was shown on the screen after each completed run, to stimulate participants to optimize their performance. The total time spent performing the tracking task was approximately ten minutes.

As the participants required some runs to converge to their optimal strategy, only the last three recorded runs were used as the final measured data. For all participants, stable performance scores were found for the last three runs. For each run, only the last 40.96 seconds were analyzed, to discard any initial control transients.

2.5 Target Forcing Function

To induce tracking errors for participants to correct and facilitate HC modeling (Mulder et al., 2018), a multisine target signal f_t was used in the experiment. The signal was generated as a sum of $N_t = 11$ sines according to:

$$f_t(t) = \sum_{k=1}^{N_t} A_t[k] \sin\left(\omega_t[k]t + \phi_t[k]\right) \tag{1}$$

In Eq. (1), A_t, ω_t, and ϕ_t represent the amplitude, frequency, and phase shift of each sine in f_t. These signal parameters were chosen similar to those used by Zaal et al. (2009), but the frequencies were adapted to a shorter measurement time (T_m) of 40.96 seconds. Where most other tracking experiments use runs of at least 90 seconds (Zaal et al., 2009), here a shorter measurement time was needed due to the vulnerable participant group.

The numerical values of all target signal properties are given in Table 2. The frequencies, ω_t, were chosen as integer multiples of the base frequency $\omega_m = 2\pi/T_m$ and evenly distributed (with logarithmic spacing) over the frequency range from 0.5 to 25 rad/s that is of interest for HC dynamics. The amplitudes A_t were set using the second-order low-pass filter of Zaal et al. (2009), to ensure a signal with attenuated power at high frequencies. The phases ϕ_t were selected from a large number of randomly generated phase sets to achieve an average crest factor.

Table 2. Target signal components

n_t,-	ω_t, rad/s	A_t, deg	ϕ_t, rad
4	0.614	1.079	7.239
7	1.074	0.776	0.506
11	1.994	0.391	7.860
17	2.915	0.225	8.184
23	4.449	0.117	9.012
29	5.676	0.082	6.141
37	6.596	0.066	6.776
53	8.130	0.051	6.265
79	12.118	0.035	4.432
109	16.720	0.028	2.672
157	24.084	0.024	8.009

2.6 HC Modeling and Identification

In a tracking task, the HC can be modeled as a quasi-linear system (Mulder et al., 2018) consisting of a linear response to perceived variables (e.g., H_{hc} in Fig. 2) and a remnant signal (e.g., n in Fig. 2) that accounts for all non-linearities in the human controller's behavior. With a multisine forcing function signal, the signal-to-noise ratio at the frequencies where this signal has power (ω_t) is very high, which enables the estimation of an HC Frequency Response Function (FRF) from measured in- and outputs:

$$\hat{H}_{hc}(j\omega_t) = \frac{U(j\omega_t)}{E(j\omega_t)} \tag{2}$$

In Eq. (2), $U(j\omega_t)$ and $E(j\omega_t)$ are the Fourier transforms of the control (u) and error (e) signals, respectively. Using the obtained FRF, the four parameters of the HC dynamics model introduced in Fig. 2 were estimated by optimizing the fit of the model's frequency response to the FRF. With the vector of estimated model parameters given as $\theta = [K_{hc}\ \tau_{hc}\ \omega_{nm}\ \zeta_{nm}]^T$, the estimated parameters were those that minimized the summed squared complex error between the FRF and the model's frequency response. This optimization problem was solved using the Matlab *fminsearch* nonlinear optimization algorithm. To avoid local minimum solutions, the optimization was ran with a hundred random initial parameter vectors, from which the best final fit was selected as the final result. For verification of the quality of the obtained model fit, the Variance Accounted For (VAF) was calculated according to:

$$\text{VAF} = \left[1 - \frac{\sum_{k=1}^{N} \|u[k] - \hat{u}[k|\theta]\|^2}{\sum_{k=1}^{N} \|u[k]\|^2}\right] \times 100\% \tag{3}$$

In Eq. (3), u and $\hat{u}$ are the measured and modeled control signal, respectively. The modeled $\hat{u}$ is obtained from simulating the fitted model for H_{hc} with the measured error signal e as input. A VAF of 100% means that the model perfectly describes the measured control signal.

2.7 Dependent Variables

To quantify and compare differences in HC behavior and performance between PD patients and controls, a number of dependent variables is presented in this paper:

- *Tracking performance and control effort.* The root-mean-square (RMS) values of the error (e) and control input (u) signals, both normalized with the RMS of the target forcing function signal f_t, were used as measures of tracking performance and control effort, respectively. The lower RMS(e)/RMS(f_t), the better participants performed the task. Furthermore, if RMS(e)/RMS(f_t) is below 1, the HC is successful in attenuating the errors induced by f_t. The higher RMS(u)/RMS(f_t) is, the larger control inputs u were on average and the more effort participants put into controlling the system.
- *HC model parameters.* The four estimated HC model parameters – K_{hc}, τ_{hc}, ω_{nm} and ζ_{nm} – are used to explicitly quantify changes in HC gain, HC delay, and NMS characteristics between patients and controls.
- *HC (non)linearity.* The VAF of the HC models is used as an indicator of HC linearity. Furthermore, the ratio of coherent output to total output is quantified using the *relative remnant* (McRuer and Jex, 1967):

$$\rho_u^2(j\omega_t) = 1 - \frac{\tilde{S}_{uu,n}(j\omega_t)}{S_{uu}(j\omega_t)} \tag{4}$$

  Eq. (4) compares the estimated remnant power ($\tilde{S}_{uu,n}$) with the total signal power (S_{uu}) at each input frequency ω_t. The relative remnant is normally between 0 and 1, where 1 indicates a perfect linear response (no remnant).

Despite the relatively low number of participants included in the data set ($n = 7$), statistical analysis was performed to compare the results for the PD patients (P) and the controls (C). Normality of collected samples was verified with a Kolmogorov-Smirnov test. For normally distributed variables an independent t-test was used to perform the comparison; otherwise a nonparametric Mann-Whitney test was applied. Significance levels were set to 0.05 and 0.01 for significant ($*$) and highly significant ($**$) between-group results, respectively.

2.8 Hypotheses

The degraded motor skills in PD were expected to result in less optimal HC control behavior in the pursuit tracking task than observed for healthy controls. Hence, the following hypotheses were formulated:

H1: *PD patients will show degraded tracking performance (higher RMS(e)/RMS(f_t)).* Degraded performance was also found in previous studies that collected tracking data from PD patients (Flowers, 1978; Hufschmidt and Lücking, 1995; Jones et al., 1996).

H2: *PD patients will show reduced HC gains K_{hc} and higher HC delays τ_{hc}.* Degraded performance in tracking tasks is associated with high HC gains and low HC delays (McRuer and Jex, 1967; Mulder et al., 2018).

H3: *PD patients' NMS dynamics will be characterized by a lower natural frequency (ω_{nm}) and increased damping (higher ζ_{nm}).* Due to reduced muscle tension (Corcos et al., 1996) and bradykinesia (slowness in movement) (Hufschmidt and Lücking, 1995), both well-known PD motor symptoms, the NMS dynamics in PD patients are expected to show reduced control bandwidth and increased damping.

H4: *PD patients' control dynamics will be less linear (lower VAF, lower ρ_u^2) than those of healthy controls.* Hand movements are generally slower for PD patients (De Boer et al., 2013), which makes it harder to react consistently, especially at high frequencies, which will result in lower HC model VAFs and reduced relative remnant ρ_u^2 compared to the controls.

3. RESULTS

3.1 Tracking Performance and Control Effort

Fig. 4 shows the results for the metrics of tracking performance (RMS(e)/RMS(f_t)) and control effort (RMS(u)/RMS(f_t)). Data from healthy controls (C) is in blue, while PD patient data (P) is shown in red. The variance bars indicate the 95% confidence intervals. Fig. 4(a) shows that the PD patients performed significantly ($U = 28.00$, $p < 0.01$) worse than the control group, with a 43% increase in RMS(e)/RMS(f_t) on average (0.78) compared to the controls (0.54). In terms of control effort, no difference was found between patients and controls ($t(12) = 0.02$, $p \geq 0.05$), see Fig. 4(b). However, the RMS(u)/RMS(f_t) data for the PD patients shows a somewhat larger spread, indicative of reduced consistency in control effort in the PD patients group.

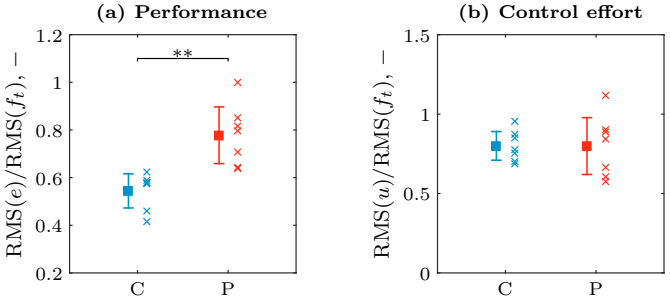

Fig. 4. Measured tracking performance and control effort.

3.2 HC Modeling Results

Fig. 5 shows the average estimated FRFs (asterisks) and fitted HC models (lines) for all PD patients and controls. It can be seen that all fitted HC models correspond well with the estimated FRFs. Furthermore, with average VAF values of 70.1% and 79.2%, respectively, the quality of fit of the HC model to the data from both patients and controls was found to be in line with similar experiments (Vos et al., 2014). As expected for the pursuit tracking task with single integrator controlled dynamics (Vos et al., 2014;

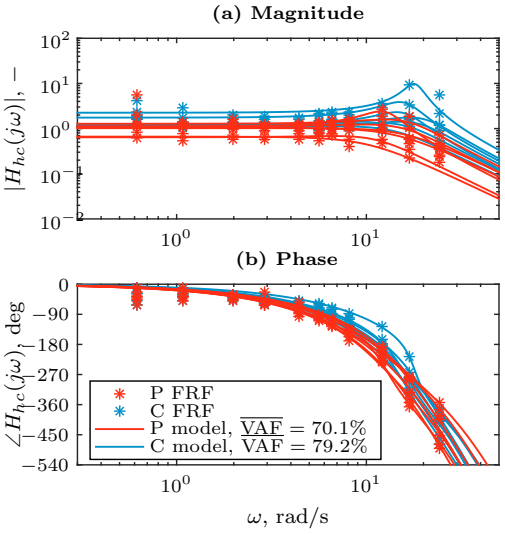

Fig. 5. FRFs and fitted HC models for all participants.

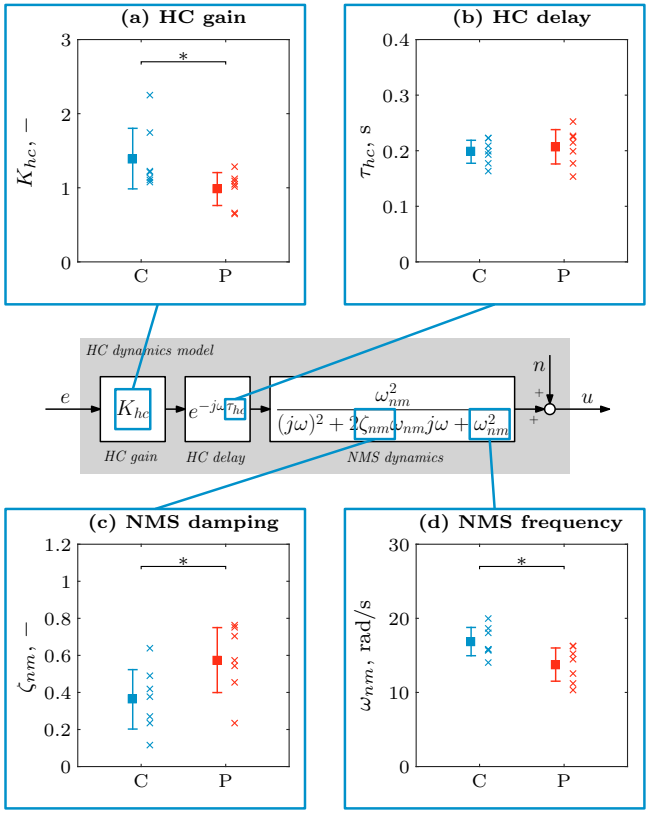

Fig. 6. Estimated HC model parameters.

Mulder et al., 2019), all participants showed proportional, gain-like, HC control dynamics. The magnitude of H_{hc} (HC gain) is clearly higher for the control group and the characteristic magnitude peak of the NMS dynamics is more pronounced. The phase roll-off with increasing frequency (see Fig. 5(b)) is not notably different in patients and controls, which suggests equivalent values of the HC delay τ_{hc} in both groups.

Fig. 6 shows the four estimated HC model parameters (K_{hc}, τ_{hc}, ζ_{nm} and ω_{nm}). Consistent with the observed FRFs in Fig. 5, Fig. 6(a) shows that the control group has a significantly higher HC gain (K_{hc}) compared to the patients ($U = 69.00$, $p < 0.05$). For the HC delay (τ_{hc}) equivalent values of around 200 ms are found for the controls and PD patients ($t(12) = -0.59$, $p \geq 0.05$), see Fig. 6(b). The marked difference in tracking performance (see Fig. 4(a)) is thus mainly attributable to a difference in HC gain. For the NMS parameters, Fig. 6(c) and 6(d) show significantly higher NMS damping ratios ζ_{nm} ($t(12) = -2.19$, $p < 0.05$) and lower neuromuscular frequencies ω_{nm} ($t(12) = 2.58$, $p < 0.05$) for the patients, respectively.

3.3 HC Nonlinearity

The results of the HC control dynamics analysis presented in Figs. 5 and 6 show significant differences between healthy controls and PD patients for the linear part of their control responses in the tracking task. Also the extent to which control behavior in the task was in fact linear was found to differ for PD patients. Fig. 7 shows the two metrics that were used to assess this linearity of the applied motor skills, i.e., the variance accounted for (VAF) and the relative remnant ratio for the control signal u.

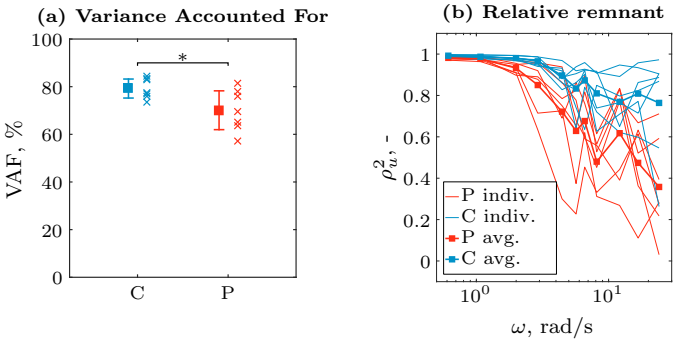

Fig. 7. Measured VAF and relative remnant.

Fig. 7(a) shows that while for both groups the fitted HC models are able to explain a high percentage of the measured control responses, the VAFs of patients are on average lower than those for the control group ($t(12) = 2.46$, $p < 0.05$). This difference implies that the linear HC model is better able to describe the control group data and thus indicates reduced linearity of the PD patients' control dynamics. This difference is further supported by Fig. 7(b), which shows the relative remnant for both groups. Data from all individual participants is presented (lines), as well as the group averages (lines with markers). For the low frequencies the data for both groups are close to unity, indicating a high degree of linearity of control at the low frequencies (McRuer and Jex, 1967). For the higher frequencies, ρ_u^2 is seen to drop and notably more for the patients (0.48 average over the highest three frequencies) than the controls (0.78 over the highest three frequencies). The VAF and relative remnant data of Fig. 7 thus shows the PD patients were less able to provide linear control.

4. DISCUSSION AND CONCLUSIONS

This paper presented the preliminary results of an effort to quantify the loss of motor skill due in PD using human controller modeling. A pursuit tracking task with single integrator controlled element dynamics was, at the time of writing of the paper, performed by seven patients and seven healthy controls. As expected (**H1**), the collected

data showed distinctly degraded tracking performance for the PD patients, consistent with earlier experiment data (Flowers, 1978; Hufschmidt and Lücking, 1995; Jones et al., 1996; Soliveri et al., 1997).

The HC modeling results revealed that PD patients used a significantly lower control gain compared to the control group (30% reduction). In contrast to earlier studies (Jones and Donaldson, 1989), the hypothesized increase in HC delay (**H2**) was not observed, thereby only partially confirming our hypothesis. For the NMS dynamics, lower natural frequencies and a higher damping ratios were expected for the PD patients (**H3**), given known motor symptoms in PD such as like bradykinesia and rigidity (Hufschmidt and Lücking, 1995). Indeed, the NMS damping was found to increase by 0.2 (58%) on average for the patients, while the NMS natural frequency was found to be around 3 rad/s (20%) lower, compared to the controls. Finally, also the expected reduced linearity of the PD patients' control dynamics (**H4**) was observed from a statistically significant 9% drop in VAF and consistently worse relative remnant (ρ_u^2). The choice to include only early-stage PD patients in the current study is a likely explanation for the absence of the hypothesized effect for the HC delay.

Despite the small group size, the data presented in this paper shows an obvious, and statistically significant, distinction in motor skills between the PD patients and controls. This in contrast to the questionnaires on cognitive functioning (MMSE and FAB), which for the same participants did not differentiate between the control group and the patients, see Table 1. For this reason, tracking tasks in combination with HC modeling techniques show clear potential as an additional diagnostic tool for direct quantification and (early) detection of the loss of motor skills due to PD. Further research will focus on optimizing the tracking task for maximizing this potential. For instance, as PD patients are known to depend more on visual information (Jones and Donaldson, 1989), a tracking task demanding increased visual processing (e.g., preview tracking) might be even more effective for quantifying the loss of eye-hand coordination and motor skills.

ACKNOWLEDGMENTS

The authors would like to thank dr. Agnita J.W. Boon for her help with participant recruitment. Furthermore, special thanks to dr. Casper de Boer and Max Keizer for their extensive help with the data collection and analysis.

REFERENCES

Corcos, D.M., Chen, C.M., Niall, P.Q., McAuley, J., and Rothwell, J.C. (1996). Strength in Parkinson's Disease: Relationship to Rate of Force Generation and Clinical Status. *Annals of Neurology*, 39(1), 79–88.

De Boer, C., Pel, J.J.M., Van den Dorpel, J.J., Boon, A.J., and Van der Steen, J. (2014). Behavioral Inhibition Errors in Parkinson's Disease Tested Using an Antisaccade and Antitapping Task. *J. of Parkinson's Disease*, 4(4).

De Boer, C., Van der Steen, J., Schol, R.J., and Pel, J.J.M. (2013). Repeatability of the timing of eye–hand coordinated movements across different cognitive tasks. *Journal of Neuroscience Methods*, 218(1), 131–138.

De Lau, L.M.L. and Breteler, M.M.B. (2006). Epidemiology of Parkinson's disease. *The Lancet Neurology*, 5(6).

Dubois, B., Slachevsky, A., Litvan, I., and Pillon, B. (2000). The FAB: A frontal assessment battery at bedside. *Neurology*, 55(11), 1621–1626.

Flowers, K.A. (1978). Some Frequency Response Characteristics of Parkinsonism on Pursuit Tracking. *Brain*, 101(1), 19–34.

Folstein, M.F., Folstein, S.E., and McHugh, P.R. (1975). "Mini-Mental State": A Practical Method for Grading the Cognitive State of Patients for the Clinician. *Journal of Psychiatric Research*, 12(3), 189–198.

Gelb, D.J., Oliver, E., and Gilman, S. (1999). Diagnostic criteria for Parkinson's disease. *Arch. of Neur.*, 56(1).

Goetz et al. (2007). Movement Disorder Society-Sponsored Revision of the Unified Parkinson's Disease Rating Scale (MDS-UPDRS): Process, Format, and Clinimetric Testing Plan. *Movement Disorders*, 22(1).

Hoehn, M.M. and Yahr, M.D. (1967). Parkinsonism: onset, progression and mortality. *Neurology*, 17(5), 427–442.

Hufschmidt, A. and Lücking, C.H. (1995). Abnormalities of Tracking Behavior in Parkinson's Disease. *Movement Disorders*, 10(3), 267–276.

Jellinger, K.A. (2001). The pathology of Parkinson's disease. *Advances in Neurology*, 86, 55–72.

Jones, R.D. and Donaldson, I.M. (1989). Tracking Tasks and the Study of Predictive Motor Planning in Parkinson's Disease. In *Annual Int. Conf. of the IEEE Engineering in Medicine and Biology Society*, 1055–1056.

Jones, R.D., Donaldson, I.M., and Sharman, N.B. (1996). A Technique for Removal of the Visuoperceptual Component from Tracking Performance and Its Application to Parkinson's Disease. *IEEE Transactions on Biomedical Engineering*, 43(10), 1001–1010.

McRuer, D.T. and Jex, H.R. (1967). A Review of Quasi-Linear Pilot Models. *IEEE Transactions on Human Factors in Electronics*, HFE-8(3), 231–249.

Muilwijk, D., Verheij, S., Pel, J.J.M., Boon, A.J., and Van der Steen, J. (2013). Changes in Timing and kinematics of goal directed eye-hand movements in early-stage Parkinson's disease. *Transl. Neurodeg.*, 2(1).

Mulder, M., Pool, D.M., Abbink, D.A., Boer, E.R., Zaal, P.M.T., Drop, F.M., van der El, K., and van Paassen, M.M. (2018). Manual control cybernetics: State-of-the-art and current trends. *IEEE Trans. on Human-Machine Sys.*, 48(5), 468–485.

Mulder, M., Pool, D.M., van der El, K., Drop, F.M., and van Paassen, M.M. (2019). Manual control with pursuit displays: New insights, new models, new issues. In *14th IFAC Symposium on Analysis Design and Evaluation of Human Machine Systems Tallinn, Estonia*, 139–144.

Soliveri, P., Brown, R.G., Jahanshahi, M., Caraceni, T., and Marsden, C.D. (1997). Learning manual pursuit tracking skills in patients with Parkinson's disease. *Brain*, 120(8), 1325–1337.

Vos, M.C., Pool, D.M., Damveld, H.J., Van Paassen, M.M., and Mulder, M. (2014). Identification of Multimodal Control Behavior in Pursuit Tracking Tasks. In *IEEE Conf. on Sys., Man, and Cybernetics, San Diego*, 69–74.

Zaal, P.M.T., Pool, D.M., De Bruin, J., Mulder, M., and Van Paassen, M.M. (2009). Use of Pitch and Heave Motion Cues in a Pitch Control Task. *Journal of Guidance, Control, and Dynamics*, 32(2), 366–377.